

# Remote camera based heart rate estimation

Dániel Terbe<sup>1</sup> and Ákos Zarándy<sup>2</sup>

<sup>1</sup> MTA SZTAKI  
terbed@sztaki.hu

<sup>2</sup> MTA SZTAKI  
zarandy.akos@sztaki.mta.hu

**Abstract.** Experimental setup for remote Photoplethysmographic measurement was built and Pulse Volume Vector based signal evaluation method was implemented to measure pulse and blood oxygenation. As opposed to the typically used RGB or three monochromatic camera, an RGB-NIR camera was applied in our setup to obtain space and time registered data from the visual and NIR regions. The setup was calibrated; the pulse and blood oxygenation curves were compared to reference signals. The real-time implementation of a state of the art method was also carried out and tested on premature infants.

## 1 Introduction

In imaging/remote photoplethysmography (iPPG, rPPG) the objective is to attain the vital signs of the patients (these are mainly the heart rate and oxygen saturation) in a remote, non-contact way, using video camera.

With our eyes we can not see color variation on our skin modulated by the heart rate<sup>1</sup>. However if a video is recorded and a RoI (Region of Interest) is averaged – this is typically a  $25 \times 25$  or  $50 \times 50$  pixel area as can be seen on Figure (1) – than a photoplethysmographic signal can be attained which contains information about the pulse, oxygen saturation and cardiovascular system. The main hardship is the SNR (Signal to Noise Ratio) which is really low in these measurements. After averaging the ROI shown in Figure (1) for each frame the raw signals are obtained which are depicted in Figure (3) and the normalized signals in Figure (4). Typically the pulsatile component is 3% of the signal in transmissive mode and even worse 0.3% in reflectance mode. A typical PPG (photoplethysmographic) waveform and the illustration of its origin is depicted on Figure (2).

The pulse can be attained most easily among the vital signs. There are many methods for extracting pulse information from the raw RGB signals of a simple camera eliminating motion and illumination induced distortions [1]. Some of the methods are functioning also in dark using near infrared cameras [7] [8] which is important for monitoring patients at night.

There are also promising attempts to measure blood oxygen saturation remotely in diffuse reflectance mode [4] [3] [5].

---

<sup>1</sup> If we fluoroscope our finger we can see pulsation.

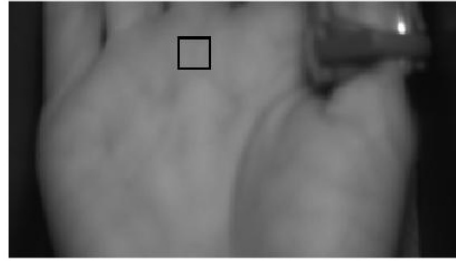


**Fig. 1.** Palm of the subject and the selected 25x25 pixel Region of Interest (ROI) which is averaged for each frame. On the thumb finger the reference pulzoximeter can be seen.

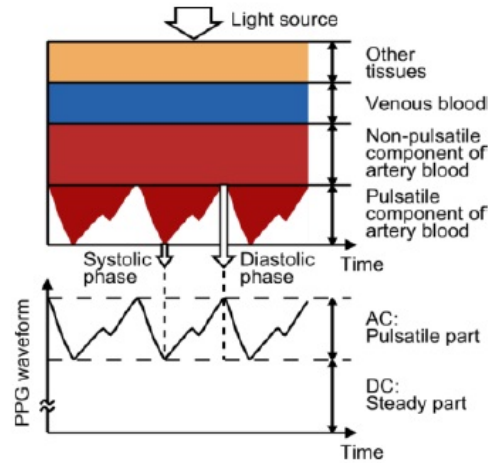


**Fig. 2.** An example of a photoplethysmographic waveform, consisting of DC and AC components. The DC component of the PPG waveform corresponds to the detected transmitted or reflected optical signal from the tissue, and depends on the structure of the tissue and the average blood volume of both arterial and venous blood. The AC component shows changes in the blood volume that occurs between the systolic and diastolic phases of the cardiac cycle; the fundamental frequency of the AC component depends on the heart rate and is superimposed onto the DC component. (reference: <http://www.seminarsonly.com/electronics/Wearable-Photoplethysmographic-Sensors.php>)

However these methods are implemented currently in offline mode, meaning that the result comes only after evaluating the previously recorded video. Actual real time testing of these methods are needed to further confirm the feasibility – real time/world applicability – of remote camera based photoplethysmography.

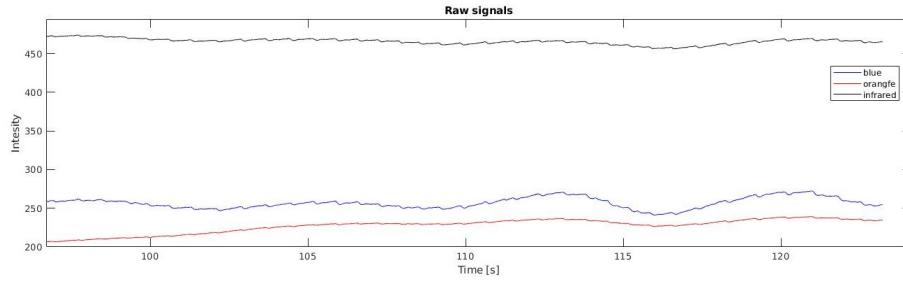


**Fig. 3.** Raw signals obtained from averaging ROI in Figure (1). (The slowly varying component is attributed to the breath.)

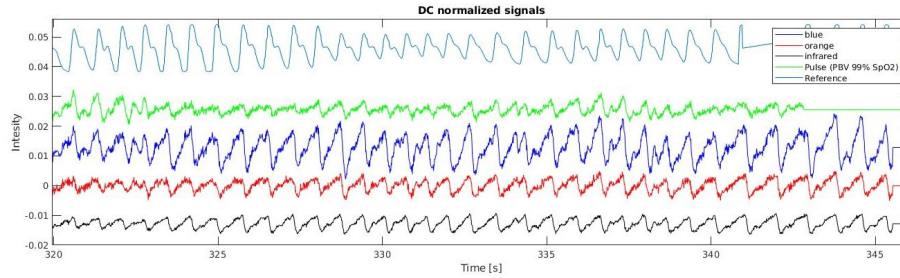


**Fig. 4.** DC normalized signals with reference signal measured with a finger pulzoximeter and computed pulse signal with PBV (Pulse Blood Volume vector) method [6].

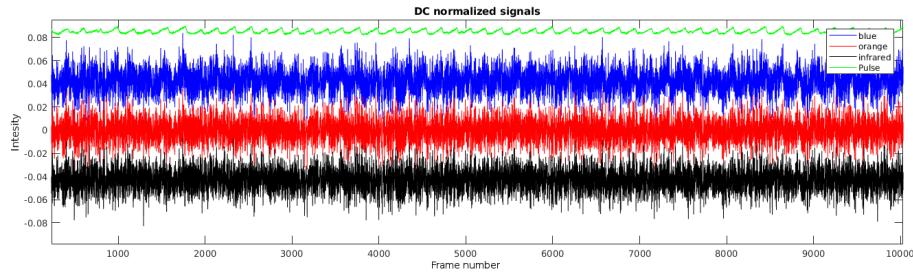


**Fig. 5.** Pulse signal extraction (green) from synthetic data with PBV method. The result is impressive because the pulse can be barely seen in the color channels (blue, red, black) but the computed pulse signal (green) is surprisingly good.

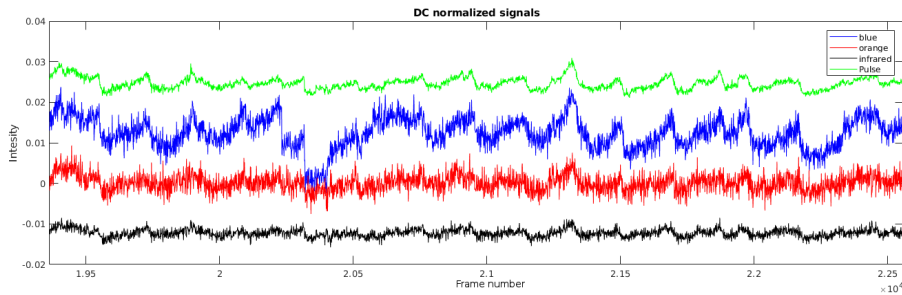


**Fig. 6.** Calculated pulse signal (green) with PBV method from recorded low quality signal (real data).

In this study we demonstrate a state of the art rPPG method and calibrate its parameters to our experimental setup. We also show the real time functioning of another method.

In the next section we will shortly introduce the PBV (Pulse Blood Volume vector) and POS (Plain orthogonal to skin) methods which are used to extract pulse from multi-channel signal.

## 2 Methods

The fundamental mathematical limitation is the following: a pulse-signal extracted by linearly combining the color-channels of an  $n$  wavelength camera can be independent of at most  $(n - 1)$  distortions. It highly restricts the rPPG performance because the SNR is low even if distortions are not present. The two main distortion in rPPG measurements are the illumination variations and the motion artifacts. Therefore at least 3 wavelengths has to be used to eliminate the main distortions. In the forthcoming part the PBV [6] and POS [1] methods will be introduced and our results of its implementation.

### 2.1 Pulse Blood Volume signature method (PBV)

We assume that the pulse-signal  $\vec{S}$  can be constructed as a linear combination of the normalized color channels  $\mathbf{C}_n$ :

$$\vec{S} = \vec{W}\mathbf{C}_n \quad (1)$$

where  $\vec{S} \in R^{1 \times N}$ ,  $\vec{W} \in R^{1 \times c}$  and  $\mathbf{C}_n \in R^{c \times N}$  where  $N$  indicates the number of samples in the time-window and  $c$  is the number of color channels. The normalized color channels are obtained in the following way:

$$C_n(i) = \frac{C(i)}{\mu(C(i))} - 1 \quad (2)$$

where  $i \in [1, c]$  represents the color channel index,  $C$  is the spatially averaged raw signal – as shown in Figure (3) – and  $\mu$  the mean in the moving time-window. Example for the result is depicted in Figure (4).

The aim is to find the weights  $\vec{W}$  that construct the pulse signal  $\vec{S}$ . De Haan *et al.* showed [6] that the optical absorption changes caused by blood volume variations in the skin occur along a very specific vector in the normalized color channel space and this is namely the Pulse Blood Volume vector  $\vec{P}_{bv}$ . This quantity depend on the physiology and on the optical system, but independent of the individuals. Therefore  $\vec{P}_{bv}$  depends on the recording system – illumination and camera properties – and the pulse signature is the same for individuals within the system. This enables robust rPPG pulse extraction that minimizes the contribution to the pulse signal of color variations with other signatures – for example motion whose signature is  $\vec{1}$  in the normalized color channel space, since it appears in all color channels equally.

The definition of  $\vec{P}_{bv}$  is the following:

$$\vec{P}_{bv}(i) \equiv \left[ \frac{AC}{DC} \right]_i \approx \sigma(C_n(i)) \quad (3)$$

where  $i$  is the color channel index,  $\sigma$  is the standard deviation in the time-window,  $AC$  is the amplitude of the signal pulsatile part and  $DC$  is the mean of the signal. As a matter of fact the components of the vector are the relative pulsatile amplitudes in the different color channels. In consequence the pulse vector  $\vec{S}$  correlation with the normalized color-channels  $\mathbf{C}_n$  proportional with  $\vec{P}_{bv}$ :

$$\vec{S} \mathbf{C}_n^T = k \vec{P}_{bv} \quad (4)$$

After substituting equation (1) into (4):

$$\vec{W} \mathbf{C}_n \mathbf{C}_n^T = k \vec{P}_{bv} \quad (5)$$

Finally we obtained the weights for the time-window:

$$\vec{W} = k \vec{P}_{bv} (\mathbf{C}_n \mathbf{C}_n^T)^{-1} \quad (6)$$

where  $k$  is the normalization factor to  $\vec{W} \vec{W}^T = 1$  be realized.

## 2.2 Remote SpO2 measurement using the blood volume pulse signature

PBV method can be adopted to measure blood oxygen saturation [4] because the relative pulsabilities of the color channels depend on the oxygenation of the blood. In consequence for every oxygenation level a blood volume signature  $\vec{P}_{bv}$  can be assigned. For every saturation level the corresponding  $\vec{P}_{bv}$  vector will present the best quality pulse signal while others will produce lower quality.

To estimate oxygen saturation, for each  $\vec{P}_{bv}$  vector the pulse signal and its SNR value are computed. The  $\vec{P}_{bv}$  resulted the highest SNR is selected and the corresponding SpO2 value is inferred as blood oxygen saturation.

The main advantage of this method is that the signal quality need to be not necessarily good, the only condition is to be able to extract heart rate, while the general Ratio of Ratios (RoR) method [9] demands good signal quality.

### 2.3 Plain Orthogonal to Skin method (POS)

In this case we project the signals into a plane which most likely contains the pulse direction (in the normalized color channel space) opposed to the PBV method where the signals were projected into a fixed vector. An ideal projection plane is the plane orthogonal to the temporally normalized skin-tone. The projected signals can be expressed in such a general form:

$$S_1(t) = d_1(t) - d_2(t) \quad (7)$$

$$S_2(t) = d_1(t) + d_2(t) - 2d_3(t) \quad (8)$$

where  $\mathbf{D} = [d_1(t), d_2(t), d_3(t)]^T$  is the normalized color channel ( $\mathbf{C}_n$ ), but in decreasing channel order regarding the relative pulsatile amplitude. Both projection axis exhibit positive pulsilities and thus generate in-phase pulse-signals.

The last step is to tune an exact projection direction within the bounded region, where the pulse signal can be further separated. We let this direction adaptively selected by the program using the following rule:

$$h(t) = S_1(t) - \alpha \cdot S_2(t) \quad \text{where} \quad \alpha = \frac{\sigma(\mathbf{S}_1)}{\sigma(\mathbf{S}_2)} \quad (9)$$

where  $\sigma(\cdot)$  denotes the standard deviation operator (in time) and  $h(t)$  is the estimated pulse signal. When the pulse dominates the signals they appear *in-phase* in  $S_1(t)$  and  $S_2(t)$ : adding two in-phase signals together will boost the resulting signal strength. In this case  $\alpha$  is non-critical. When the specular component dominates, they appear *anti-phase* and  $\alpha$  can pull/push the variation strength of one signal to the same level as the other one. Adding two anti-phase signals together with the same amplitude will cancel out the specular distortion. We have to note that its performance becomes sub-optimal when the pulsatile strength and specular strength are very close to each other.

The main advantage of this method is that it adapts to different illumination and camera setups, no calibration is needed.

### 3 Results

#### 3.1 Experimental set up

**Offline** In the offline experiments we used  $440nm$ ,  $600nm$  and  $850nm$  LED illumination with an RGB-IR camera. The used camera model was *e-CAM40*<sup>2</sup>. In regular RGB cameras, one color pixel quad is composed from one red, two greens and one blue color channels. It automatically solves the spatial and temporal matching, which arises immediately when two cameras are used. In this camera we have an additional infrared channel that enables us to record simultaneously another chromatic channel from  $800nm - 1000nm$  which is favorable regarding oximetry purposes. In our experimental setup, this camera streams  $672 \times 380$  unprocessed 10-bit RAW data video upto 100 fps with  $10ms$  exposure time. The recordings were conducted on the members of our laboratory.

**Online** In the real-time measurements we tested more RGB cameras and also a three monochrome camera installment with the following filters:  $750nm$ ,  $800nm$ ,  $900nm$ . The used camera models: Basler acA2040-55uc color and Basler acA2040-55um monochrome cameras.

The image stream is recorded with  $500 \times 500$  pixel resolution, 12 bit pixel depth and 20 frame per seconds.

#### 3.2 Pulse extraction using the blood volume pulse signature

We obtained the pulse blood volume signature  $\vec{P}_{bv}$  (at 99% oxygen saturation) for our recording system. To achieve that we computed the relative pulsatile amplitudes of the color channels ( $440nm$ ,  $600nm$ ,  $850nm$ ) for each RoI cell – that resulted a good signal quality – with a 10 second moving time-window and finally calculated its average and standard deviation:

$$\vec{P}_{bv}^{99\%} = (0.90 \pm 1\% \ 0.33 \pm 3\% \ 0.27 \pm 7\%)$$

After that we tested the method on synthetic data which is illustrated in Figure (5) and on a recorded low quality signal that is shown in Figure (6). The synthetic data was constructed by adding the same gaussian white noise to each color channel of a good quality signal, that way simulating motion artifact<sup>3</sup> – since it appears equally in each channel.

<sup>2</sup> e-CAM40\_CUMI4682\_MOD: <https://www.e-consystems.com/OV4682-RGB-IR-MIPI-CAMERA-Module.asp>

<sup>3</sup> However its frequency is much larger than motion induced variation, but for the sake of illustration it is adequate.

### 3.3 SpO2 measurement using the blood volume pulse signature

We conducted oxygen saturation measurements with reference pulzoximeter. The subjects were asked to hold they breath and decrease their oxygen saturation level and after around 1 minute start breathing again. The reference pulzoximeter moved in range 68% – 100%. The decreasing (95% → 70%) and also the increasing parts (70% → 99%) were recorded.

We computed the general Ratio of Ratios using 2 color channels in a 10 second moving window with a step size of 1 second for each good quality RoI (illustration in Figure (7)) and calculated the spatial mean value:

$$R = \frac{(AC/DC)_1}{(AC/DC)_2} \quad (10)$$

and examined its correlation with the reference  $SpO_2$  which is depicted on Figure (8). Also the relative pulsabilities – expressed in equation (3) – were calculated for each color channel which is shown in Figure (9).



**Fig. 7.** Illustration of the spatial signal quality.

Based on the results illustrated in Figure (9) a calibration curve is constructed for the pulse blood volume vector  $\vec{P}_{bv}(SpO_2)$  which is depicted in Figure (10).

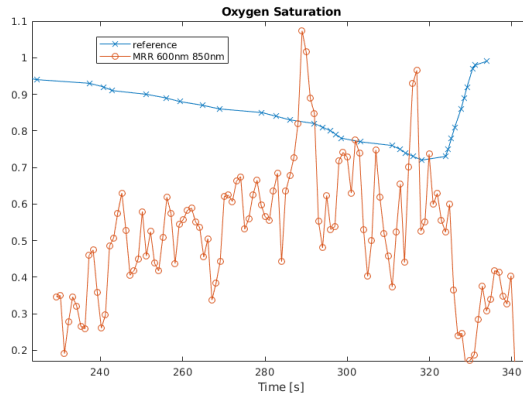


**Fig. 8.** The reference SpO2 values and the calculated Ratio of Ratios. Inverse correlation can be seen covered by significant noise.

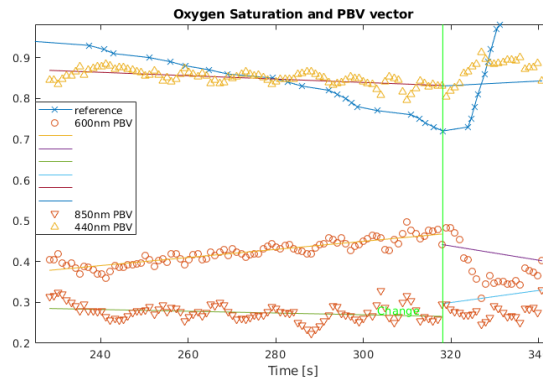


**Fig. 9.** The reference pulzoximeter SpO2 values illustrated with the relative pulsabilities of the color channels and linear fit to data. The vertical green line denotes the end of the breath holding event.

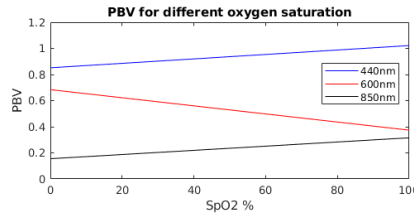


**Fig. 10.** PBV vector elements assigned to different oxygen saturation values obtained by liner fit to data and normalization.

### 3.4 Real-time remote heart rate estimation using Plane Orthogonal to Skin (POS) method

We constructed the online system based on the Full Video Pulse Extraction (FVP) method [1], where the subregions are grouped based on the color feature. The skin regions are selected where pulse can be found and combined into a final pulse signal. The advantage of this method is that we don't have to define and track a ROI, what is essential for long-term monitoring. For pulse extraction we used the Plain Orthogonal to Skin method (POS).

We implemented the real-time system in python and also in c++ using OpenCV libraries. The program is tested on the members of our laboratory and also on premature infants. The results were compared to reference: our system predicted successfully the heart rate in the cases where significant subject motion was not present. On figure (11) a photo can be seen from the online measurement of an infant (using our python implementation). The c++ interface is depicted on figure (12). Both implementation can process the data at 20fps.



**Fig. 11.** Real-time remote pulse monitoring of premature infant. The predicted Heart Rate in this case is 180bpm which is approved by reference.

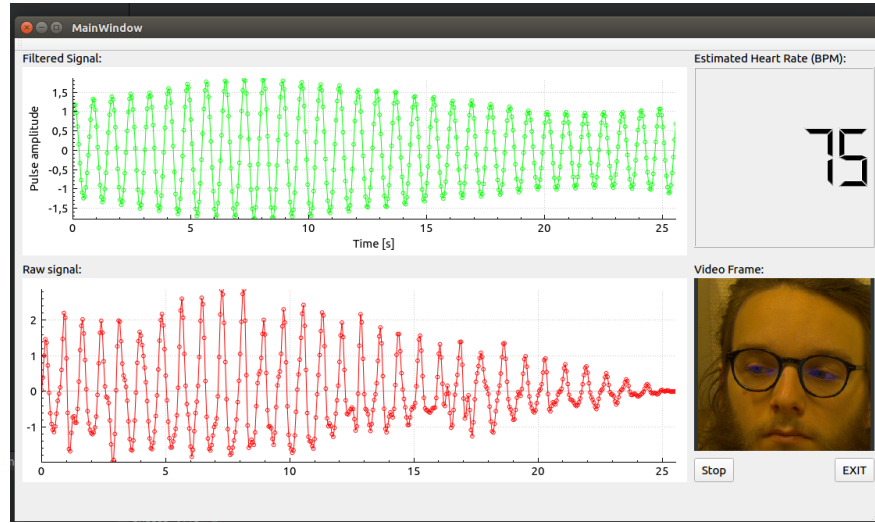


**Fig. 12.** The interface of the c++ program.

## 4 Summary

We introduced and demonstrated the functioning of a recent method (PBV [6]) which is used to attain pulse and oxygen saturation information from multi-channel rPPG signal. We tested its capabilities in extracting pulse signal from noisy data. For that we obtained the pulse blood volume vector for our recording set-up regarding 99% blood oxygenation. We also computed the calibration diagram  $\vec{P}_{bv}(SpO_2)$  in order to employ the method to estimate oxygen saturation, which is our next step in the future plan.

We also constructed a real-time implementation of the Plane Orthogonal to Skin (POS [1]) method using the Full Video Pulse extraction (FVP [1]) method in place of RoI tracking and showed the feasibility of online monitoring remotely. However further validation is needed.

Our next plan is to create a large database containing video recordings from premature infants and reference vital signs to be able to further improve and test the efficiency of different methods. Finally we want to station a complex real-time infant monitoring system and compare its results to the reference online.

## Acknowledgement

This work was supported by the Hungarian VEKOP 2.2.1-16-2017-00002 grant, titled "New intelligent digital resuscitation table (open incubator) development for neonatal and premature infants to reduce their mortality rate and increase their chances of a healthy life".

## References

1. Wang, W. Robust and automatic remote photoplethysmography. Diss. Technische Universiteit Eindhoven, 2017.
2. Corral, Francisco, Gonzalo Paez, and Marija Strojnik. "A photoplethysmographic imaging system with supplementary capabilities." *Optica Applicata* 44.2 (2014).
3. Verkruyse, Wim, et al. "Calibration of contactless pulse oximetry." *Anesthesia and analgesia* 124.1 (2017): 136.
4. Van Gastel, Mark, Sander Stuijk, and Gerard De Haan. "New principle for measuring arterial blood oxygenation, enabling motion-robust remote monitoring." *Scientific reports* 6 (2016): 38609.
5. Van Gastel, Mark, Sander Stuijk, and Gerard De Haan. "Camera-based pulse-oximetry-validated risks and opportunities from theoretical analysis." *Biomedical optics express* 9.1 (2018): 102-119.
6. De Haan, Gerard, and Arno Van Leest. "Improved motion robustness of remote-PPG by using the blood volume pulse signature." *Physiological measurement* 35.9 (2014): 1913.
7. van Gastel, Mark, Sander Stuijk, and Gerard de Haan. "Motion robust remote-PPG in infrared." *IEEE Transactions on Biomedical Engineering* 62.5 (2015): 1425-1433.
8. van Gastel, Mark, et al. "Near-continuous non-contact cardiac pulse monitoring in a neonatal intensive care unit in near darkness." *Optical Diagnostics and Sensing XVIII: Toward Point-of-Care Diagnostics*. Vol. 10501. International Society for Optics and Photonics, 2018.
9. Severinghaus, John W. "Takuo Aoyagi: discovery of pulse oximetry." *Anesthesia & Analgesia* 105.6 (2007): S1-S4.